

near the Pacific coast of Nicaragua. The quiet zone lies within a region indicated by the seismic gap technique to be a likely location for an earthquake of magnitude 7 or larger within the next few decades. Teleseismic data show that the quiescence has existed since at least 1950 and that the quiet zone appears to have been last ruptured by a magnitude 7.5 earthquake in 1898. Because the rupture zones of large earthquakes are observed to be seismically quiescent for years to decades prior to the main shock, the quiet zone in Nicaragua may be the site of a future large earthquake. A rough estimate of the magnitude of an earthquake that would rupture the entire quiet zone indicates that it could be comparable to the magnitude 7.5 event in 1898.

An increase in the level of seismicity in the magnitude range 3.5 to 5.0 occurred along the edges of the quiet zone in mid-1977 and continued through 1978. The distribution of earthquakes of magnitude 5.0 and larger for the same time period, however, is not significantly different from the overall distribution of earthquakes larger than magnitude 5.0 since 1950. Thus it is not known whether the increase in the number of magnitude 3.5 to 5.0 events is a normal fluctuation in lower magnitude seismicity or part of a precursory pattern. Moreover, observed precursory seismicity patterns vary and their use as a predictor is still in the development stage. We feel, therefore, that although the data clearly show a seismic quiet zone that is a possible location for a future large earthquake, they do not yet enable forecasting of such an earthquake within a specific time frame.

DAVID H. HARLOW
RANDALL A. WHITE

INES LUCIA CIFUENTES

U.S. Geological Survey,
Menlo Park, California 94025

ARTURO ABURTO Q.
Instituto de Investigaciones Sísmicas,
Managua, Nicaragua

References and Notes

1. J. A. Kelleher, L. R. Sykes, J. Oliver, *J. Geophys. Res.* **78**, 2547 (1973).
2. W. R. McCann, S. P. Nishenko, L. R. Sykes, J. Krause, *U.S. Geol. Surv. Open-File Rep. 78-943* (1978), p. 441.
3. K. Mogi, *Bull. Earthquake Res. Inst. Tokyo Univ.* **47**, 395 (1969); J. A. Kelleher and J. Savino, *J. Geophys. Res.* **80**, 260 (1975).
4. M. Ohtake, T. Matumoto, G. V. Latham, *Pure Appl. Geophys.* **115**, 375 (1977).
5. A. Aburto, *Bull. I.I.S. (Inst. Invest. Sísmicas) Managua, Nicaragua 1* (1975).
6. P. Molnar and L. R. Sykes, *Geol. Soc. Am. Bull.* **80**, 1639 (1969); B. W. Dean and C. L. Drake, *J. Geol.* **86**, 111 (1978).
7. S. K. Singh, J. Havskov, L. Ponce, K. McNally, L. Gonzalez, *Earthquake Notes* **49**, 49 (1979).
8. M. J. Carr and R. E. Stoiber, *Geol. Soc. Am. Bull.* **88**, 151 (1977).

9. J. W. Dewey and S. T. Algermissen, *Bull. Seismol. Soc. Am.* **64**, 1033 (1974).
10. H. Kanamori and K. Abe, *J. Geophys. Res.* **84**, 6131 (1979).
11. J. Crawford, *Am. Geol.* **22**, 56 (1898).
12. F. Montessus de Ballore, *Tremblements de Terre et Eruptions Volcaniques au Centre-Amérique Depuis la Conquête Espagnole Jusqu'à Nos Jours* (Société des Sciences Naturelles de Saône-et-Loire, Dijon, 1888).
13. M. Ohtake, T. Matumoto, G. V. Latham, *Bull. I.I.S. (Inst. Invest. Sísmicas) Earthquake Eng.* **15**, 105 (1977); E. R. Engdahl, *U.S. Geol. Surv. Open-File Rep. 79-943* (1978), p. 163; L. M. Jones and P. Molnar, *J. Geophys. Res.*, in press; M. Reyners, in *3rd Maurice Ewing Symposium—Earthquake Prediction*, D. W. Simpson and P. G. Richards, Eds. (American Geophysical Union, Washington, D.C., in press), vol. 4.
14. P. Molnar, *Bull. Seismol. Soc. Am.* **69**, 115 (1979).
15. L. R. Sykes and R. C. Quittmeyer, *Eos* **60**, 884 (1979).
16. J. B. Minster and T. H. Jordan, *J. Geophys. Res.* **83**, 5331 (1977).
17. H. Kanamori, *ibid.* **82**, 2981 (1977).
18. L. A. Wyllie, Jr., R. N. Wright, M. A. Sozen, H. J. Kegenkolb, K. V. Steinbruggen, S. Kramer, *Bull. Seismol. Soc. Am.* **64**, 1069 (1974).
19. We thank A. G. Lindh, W. Thatcher, P. L. Ward, and D. M. Boore for critically reading this report. We especially thank D. Fajardo and co-workers at the Instituto de Investigaciones Sísmicas in Managua for their diligence in maintaining the seismic network and analyzing the seismograms.

11 February 1981

Spectral Analysis of Tropospheric Aerosol Measurements Obtained with a New Fast Response Sensor

Abstract. A new fast response sensor was used in aircraft studies of fluctuations in the size distributions of tropospheric aerosol and their relation to fluctuations of trace gas concentrations and light scattering coefficients. Spectral analysis of data upwind of Buffalo, New York, and Houston, Texas, suggests important roles for atmospheric turbulence and chemical reaction in aerosol fluctuations.

Essential information on the dynamical processes governing the tropospheric aerosol is contained in the smaller scale spatial and temporal fluctuations in the particle size distribution. Despite extensive investigations of the tropospheric (principally urban) aerosol over the past decade [for example (1)], these fluctuations and their relation to fluctuations in trace gas concentrations and light transmission have received little attention. In this report we present a detailed analysis of these phenomena that was made possible by our development of an instrument called the electronic cascade impactor (ECI) to obtain information on the aerosol size distribution in real time (2). The measurement systems used in our aircraft studies and the spectral techniques employed in our analysis are briefly described. Typical conditions and a few representative results are given for the spectral relation among aerosol size fractions, trace gas concentrations, and light scattering coefficients.

The data for the spectral analyses were obtained from separate field studies in Buffalo, New York, during 24 to 31 March 1980 and Houston, Texas, during 5 to 15 June 1980. Although different aircraft were used, the quantities measured were the same: particle size distribution (ECI channels), trace gas concentration (SO₂, O₃, NO_x, NO, NO₂), light scattering coefficient b_s (integrating nephelometer), pressure, and temperature. Data were digitized and recorded by data acquisition systems. All instruments, with the exception of the ECI, met Environmental Protection Agency (EPA) standards and were calibrated dai-

ly by standard procedures. The ECI was calibrated in the laboratory before and after each study; no changes were found in calibration.

In these studies the ECI permits determination of a large portion of the aerosol size distribution with response times under 1 second. In the ECI, aerosol particles acquire a positive electric charge from a corona charger. They then enter a multistage cascade impactor in which each impaction stage and the final filter are isolated electrically from other parts of the impactor and connected to an electrometer amplifier. Particles are collected on surfaces at different stages according to their aerodynamic diameter, as in an ordinary impactor, but the currents arising from the deposited charge can be measured, amplified, and recorded in real time and converted through suitable inversion techniques to give particle size distributions. Since a detailed description of the ECI was published (2), some changes in the instrument have been made. The ECI now in use is a seven-channel instrument having six impaction stages and a final filter. Impaction stages 1 through 6 have 50 percent aerodynamic cutoff diameters, D_{50} 's, of 9.6, 2.9, 1.1, 0.7, 0.42, and 0.25 μm , respectively, while the final filter (ECI channel 7) gives the particle concentration below 0.25 μm and correlates well (correlation coefficient, $r = .95$) with a condensation nuclei counter (2).

Spectral analysis is a useful technique for examining the data from these aircraft field studies. While calculations of the mean, variance, auto-, and cross-correlation for the measured quantities

yield important information about spatial and temporal variations, computation of spectral density functions yields additional information derived from the frequency composition of the data. For short flight segments the data may be assumed to be stationary and the application of spectral analysis to observations along a line, rather than with time as the independent variable, is justified (3). We have carried out digital auto- and cross-power spectral analysis for crosswind flight data with up to 512 data points per channel. During the same portion of a flight, the autopower spectral density is obtained for each channel, and for each combination of two channels the magnitude of the transfer function, phase spectrum, and (squared) coherence spectrum are calculated. The autopower spectral density function gives the general frequency composition of random data in terms of the spectral density of the mean square value and is the Fourier transform of the autocorrelation function (4). In cross-power spectral analysis, our major interest is the squared coherence spectrum for two quantities. The squared coherence function is a real-valued quantity varying between zero and one and is a measure of the degree of coherence or correlation squared at a given frequency (5).

During the Buffalo study, skies were overcast, the surface wind speed was about 4 m/sec, and a neutral temperature layer was usually found from the surface up to the cloud base. The aircraft used was a UH-1H helicopter operated for the EPA. Crosswind flights were carried out at a constant height of ~ 220 m above ground level with a constant airspeed of 34 m/sec. Two sampling lines were used—one for the ECI, the other for the trace gases and nephelometer. Each sampling inlet was located on the side of the helicopter forward of the rotor wash and away from skin flow. Data were digitized and stored by two Datel Data Loggers at a sampling rate of one set of data every 2 seconds.

For crosswind flights in Buffalo remote from major localized sources, log-log plots of the autopower spectral densities for the ECI channels, b_s , and trace gas concentrations were linear for frequencies greater than approximately 0.01 Hz and exhibited slopes in the range -1.65 to -1.75 , in close agreement with a predicted slope of $-5/3$ from turbulence (3). Observed ozone concentrations, $[O_3]$, were low, usually below 10 parts per billion, and data both upwind and downwind of local sources show negligible coherence between all ECI

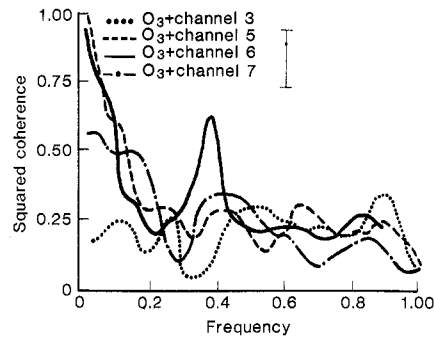


Fig. 1. Squared coherence between ozone concentration and ECI channels for upwind flights in the Houston area. Frequency is given as a fraction of the Nyquist frequency (0.5 Hz). The error bar shows the 90 percent confidence interval for a squared coherence of 0.9.

channels and $[O_3]$. Negligible coherence between other trace gas concentrations and the ECI channels was also obtained.

During the Houston study, there was no significant cloud cover, surface winds were 5 to 10 m/sec, and daytime conditions were unstable with strong surface heating. The aircraft used was a twin-engine Navajo operated by the Radian Corporation. The daytime crosswind flights reported here were at a constant height of ~ 300 m above ground level and a constant airspeed of 58 m/sec. The single sampling train had an inlet atop the plane away from the propeller and skin effect. Air was first drawn into the ECI through an isokinetic probe at the rate of 1.5 liter/sec, and the remaining air was sampled by the trace gas instruments and then passed through the nephelometer. Data were digitized and stored by a Radian Dart II data acquisition system at a rate of one complete set per second.

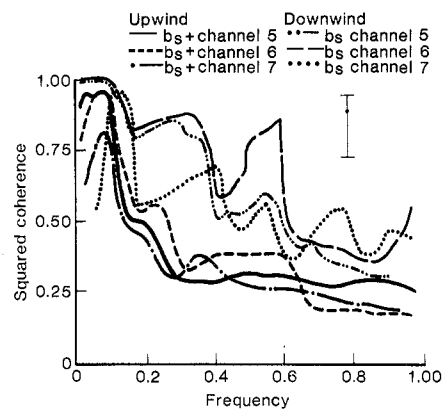


Fig. 2. Squared coherence between b_s and ECI channels for crosswind measurements in the Houston area. Frequency is given as a fraction of the Nyquist frequency (0.5 Hz). The error bar shows the 90 percent confidence interval for a squared coherence of 0.9.

For daytime crosswind flights in Houston downwind of urban and industrial sources, log-log plots of the autopower spectral densities for the ECI channels, b_s , and trace gas concentrations were linear with slopes different from the predicted $-5/3$; the slopes varied from -1.5 to -3.0 , as would be expected under the prevalent convective conditions. Similar plots for flights upwind of the urban-industrial areas of Houston (but downwind of the coastal regions southeast of Houston) showed similar behavior. However, for these upwind flights, the spectral densities for ECI channels 4 to 6, b_s , and $[O_3]$ did not exhibit linear plots at higher frequencies, but showed strong peaks at frequencies above 0.3 Hz; additional studies will be required to explain these results. The remaining ECI channels and trace gas concentrations yielded linear plots at higher frequencies with no peaks. For Houston, $[O_3]$ was relatively high; even upwind measurements showed mean values near 0.1 ppm with peak values greater than 0.2 ppm. While data from crosswind Houston flights immediately downwind of sources show negligible coherence between all ECI channels and $[O_3]$, upwind flights show that there is coherence near unity between $[O_3]$ and ECI channels 5 and 6 ($D_{50} = 0.42$ and $0.25 \mu\text{m}$, respectively) for a limited low-frequency band, and negligible coherence for $[O_3]$ and the other ECI channels. These results are shown in Fig. 1. Other trace gas concentrations showed negligible coherence with these and the remaining ECI channels. These results imply secondary aerosol production involving ozone but not SO_2 , NO , or NO_2 . Hydrocarbons, which were not measured, are hypothesized to be the secondary aerosol source.

It has been suggested (1) that there is a high correlation between b_s and the urban aerosol mass concentration in the particle diameter range 0.1 to $2 \mu\text{m}$, the so-called fine particle mass. The validity of this suggestion was tested by calculating the coherence between b_s and the ECI channels for both upwind and downwind flights. Typical results for Houston are shown in Fig. 2. While the coherence between b_s and ECI channels 5 and 6 is near unity for a limited low-frequency band, it is not statistically significant for b_s and other impactor channels. This implies that the correlation between b_s and urban aerosol mass concentration is most significant over larger distance scales in the particle diameter range ~ 0.2 to $0.5 \mu\text{m}$. However, for flights immediately downwind of industrial

sources, fluctuations in the aerosol size distribution are governed by the nearby sources and coherence near unity between b_s and nearly all ECI channels may be found for a fairly broad low-frequency band, although again the coherence is greatest and the band broadest for ECI channels 5 and 6.

The ECI has enabled us to carry out aircraft studies of fluctuations in the size distribution of tropospheric aerosol and of the relation of these fluctuations to those of trace gas concentrations and light scattering coefficients over Buffalo and Houston. Spectral analysis of the crosswind flight data upwind of industrial and urban sources in Buffalo indicates that most of the observed fluctuations were associated with atmospheric turbulence. Similar analysis of data from

Houston suggests, among other features, secondary aerosol formation associated with ozone.

R. J. TROPP

J. R. BROCK, P. J. KUHN

Department of Chemical Engineering,
University of Texas, Austin 78712

References and Notes

1. G. Hidy, P. Mueller, D. Grosjean, B. Appel, J. Wesolowski, *The Character and Origins of Smog Aerosols* (Wiley, New York, 1980).
2. R. Tropp, P. Kuhn, J. Brock, *Rev. Sci. Instrum.* **51**, 516 (1980).
3. B. F. Pasquill, *Atmospheric Diffusion* (Van Nostrand, London, ed. 2, 1974).
4. G. Jenkins, *Appl. Stat.* **14**, 2 (1965).
5. J. Bendat and A. Piersol, *Random Data* (Wiley, New York, 1971).
6. This work was supported by the Aerosol Research Branch, U.S. Environmental Protection Agency. We thank E. J. Powers and Y. C. Kim for their advice and assistance with the spectral analysis.

13 January 1981; revised 17 April 1981

Isolation of Biological Materials by Use of Erbium (III)-Induced Magnetic Susceptibilities

Abstract. Positive magnetic susceptibilities can be introduced into biological materials by their sequestration of erbium (III) ions. Particles of such material may then be manipulated under the influence of an external magnetic field.

With the increasing use of magnetism for analysis, separation, and purification and the prospect of directing drugs to specific body locations under the influence of a magnetic field (1), ways of artificially introducing positive magnetic susceptibilities in otherwise diamagnetic materials warrant attention. The ability to do this selectively and in a predictable, controlled manner is especially desirable. Magnetic techniques have been used to separate red cells from whole blood (2, 3), recover specific cell types from heterogeneous mixtures with magnetic antibody complexes (4, 5), and rapidly purify enzymes by use of affinity ligands bound to magnetic beads (6). Here we report the effectiveness of Er^{3+} as a magnetizing agent.

Preliminary observations by Westcott (7) indicated that large positive susceptibilities can be introduced in biological particles by their adsorption of magnetic cations (8). Such "magnetized" particles can then be easily manipulated by magnetic fields. The trivalent cations of the lanthanide series are especially effective in this respect. Owing to the presence of unpaired f electrons, these cations have some of the highest magnetic moments of any individual ions (Er^{3+} , 9.5 Bohr magnetons; Ho^{3+} , 10.3 Bohr magnetons). In addition, their large charge-to-radius ratio results in strong affinities for

suitable negatively charged ligands. In the work reported here we magnetized a variety of substances by binding Er^{3+} to anionic moieties in the target material. Particles of materials that have been magnetized in this way can be retrieved from suspension under the influence of an external magnetic field.

The principles underlying such magnetic separations can be easily demonstrated by adding a small quantity of beaded cation-binding resin to a solution of 1 to 10 mM ErCl_3 . In the absence of Er^{3+} , the beads show no magnetic behavior. With Er^{3+} in the solution, they are strongly attracted to a magnet placed against the sides of the container.

The forces on a particle suspended in a magnetic field involve complex mathematics, even for relatively simple geometries. Such expressions may, however, be generalized for a particle in a medium where the magnetization of neither the particle nor the medium is large compared to the magnetic field strength, H . Computation is simplified by considering only the z component of force due to the z component of the field gradient. With these assumptions, the force in the direction of the magnetic gradient on a particle immersed in a fluid can be adequately described by

$$F_z = (\psi_f - \psi_p) H_z \frac{\delta H_z}{\delta z} \quad (1)$$

where ψ_p and ψ_f are the magnetic susceptibilities of the particle and the fluid, respectively, and H_z ($\delta H_z / \delta z$) is the volume average of the corresponding product (9). Thus, neglecting any hydrodynamic and gravitational forces, a particle with a magnetic susceptibility ψ will experience a force equal to the difference between the ψ of the medium and that of the particle, times H , times the gradient of the field strength over the volume of the particle.

In the simple demonstration described above, the cation-binding particles are normally diamagnetic. Hence the positive magnetic susceptibilities observed must arise from adsorption of paramagnetic Er^{3+} ions from solution. Considering Eq. 1, the attraction of these particles by magnetic fields indicates that the concentration of Er^{3+} cations about the particles is greater than that of a corresponding volume of solution. Preliminary experiments with a torsion magnetometer have indicated that mutual alignment of the electron spins of adsorbed Er^{3+} , which would produce domains of pseudoferrromagnetism, does not occur. The resulting positive magnetic moment should therefore be proportional to the sum of the moments of the individual Er^{3+} ions bound to each particle.

The relation between magnetic forces and adsorbed paramagnetic cations can be explored, without complex mathematical treatments, by ferrography, a well-characterized technique for magnetic separations (10). The principles of the ferrographic method are illustrated in Fig. 1. The relative volume magnetic susceptibility of a particle can be determined by the distance (millimeters) it travels along a glass slide in the presence of a restraining perpendicular magnetic force. In this fashion, the relative magnetic susceptibility of each component of a mixture of particles can be assessed while separating the components on the basis of their magnetic behavior.

In the application described here, the adsorption of the paramagnetic cation Er^{3+} by several types of cation-binding material was employed to demonstrate the principles of induced magnetic moments. Hydroxyapatite, Dowex 50W, and carboxymethyl cellulose were selected as model particles. Cellulose particles served as a reference, since their Er^{3+} binding would be minimal under the conditions used. The extent of Er^{3+} binding by equal weights of each material in 150 mM KCl, pH 6.0, was determined by the murexide technique over a range of initial Er^{3+} concentrations from